Vortex-Free State of ^{3}He-B in a Rotating Cylinder

P. J. Hakonen and K. K. Nummila
Low Temperature Laboratory, Helsinki University of Technology, SF-02150 ESPOO 15, Finland
(Received 13 April 1987)

Vortex-free states have been observed in ^{3}He-B at rotation speeds up to 0.9 rad/s in a cylinder of 5-mm diameter. The measured cw NMR spectra, reflecting the order-parameter structure, respond very differently to rotation in opposite directions. The sign of this asymmetry is not linked to the direction of the applied magnetic field, as expected for a gyromagnetic effect, but varies randomly from one cooldown to another.

PACS numbers: 67.50.Fi

The superflow properties of ^{3}He-B are, on the whole, similar to those of ^{4}He-II. A remarkable difference, however, is the coupling of the B-phase order-parameter texture with the superfluid flow, which has been studied recently;[1,2] general agreement with theory[3,4] has been established.

We have investigated vortex-free counterflow states in ^{3}He-B at 29.3 bars in a rotating cylinder of radius $R=2.5$ mm; cw NMR at 923 and 1653 kHz was used. The experimental volume was similar to that in our previous experiments,[1] except that the height of the cylinder was reduced by 5 to 25 mm and a Mylar diaphragm, with a 1.5-mm hole, was installed to separate the cylinder from the heat-exchanger volume ($\phi=30$ mm). Originally, the diaphragm was inserted to elucidate vortex creation in the A phase. Its effect, however, was much more pronounced in ^{3}He-B. The diaphragm increased the critical angular velocity Ω_c for vortex formation from the previously measured[1] value of 0.1–0.2 rad/s to 0.4–0.5 rad/s at 284 Oe and to 0.9 rad/s at 504 Oe. Thus, vortices created below the diaphragm in the heat-exchanger volume did not move freely through the 1.5-mm hole to fill the sample volume.

These large values of Ω_c made is possible to undertake a study of the intrinsic orbital angular momentum of ^{3}He-B in an external magnetic field. There are two different views on this: (1) The intrinsic orbital angular momentum $L_i=-R_{ai}S_a$ is a bulk property,[5] giving rise to a free-energy term $-\boldsymbol{\Omega}\cdot\mathbf{L}=(\chi/\gamma)\boldsymbol{\Omega}\cdot\mathbf{R}\cdot\mathbf{H}$, where $\mathbf{R}(\hat{\mathbf{n}},\theta)$ is the rotation matrix defining the B-phase order parameter and $\mathbf{S}=(\chi/\gamma)\mathbf{H}$ is the spin produced by the field. (2) The intrinsic orbital angular momentum transforms into a surface current[6] yielding, in our case, a surface free-energy term $F_{gm}^s=\frac{4}{5}\kappa_s a\hat{\boldsymbol{\Omega}}\cdot\mathbf{R}\cdot\mathbf{H}$, where κ_s is proportional to the surface magnetization. Previously it was proposed[7] to measure κ_s in small tubes of 0.5-mm diameter during the transient period after rotation has been started but before vortices have formed. However, the increased value of Ω_c in a relatively large cylinder makes the comparison between these two viewpoints more advantageous in the present geometry.

In a magnetic field of about 300 Oe, the B phase in a nonrotating cylindrical geometry forms the so-called flare-out texture which has been extensively studied both experimentally and theoretically.[8] This configuration results from a balance between the magnetic anisotropy energy $F_M=-a(\hat{\mathbf{n}}\cdot\mathbf{H})^2$, gradient energy, and the surface-field energy $F_s=-d(\hat{\mathbf{s}}\cdot\mathbf{R}\cdot\mathbf{H})^2$, where $\hat{\mathbf{s}}$ is the surface normal. Usually F_s is considered large and the boundary condition $\alpha=60°$ for the azimuthal angle and $\beta=63.4°$ for the inclination angle are taken as fixed

$$(\hat{\mathbf{n}}=-\sin\beta\cos\alpha\hat{\mathbf{r}}+\sin\beta\sin\alpha\hat{\boldsymbol{\phi}}+\cos\beta\hat{\mathbf{z}}).$$

The data to be presented in this paper show, however, that this is not strictly true and that a large counterflow significantly modifies the orientation of $\hat{\mathbf{n}}$ at the boundary.

When the cylinder is rotated, the normal fluid is set into rotation while the superfluid remains stationary, resulting in a spatially varying counterflow state with $v_s-v_n=-\Omega r$, where r is the distance from the cylinder axis. This will modify the texture mainly through the flow-field free-energy term $F_{vH}=-\frac{2}{5}a[(\mathbf{v}/v_c)\cdot\mathbf{R}\cdot\mathbf{H}]^2$, where $v_c=(g_D/\rho_s)^{1/2}$, g_D is the dipolar energy coefficient, and ρ_s is the superfluid density. The texture in this case has been studied by Volovik *et al.*,[9] who show that, when ΩR slightly exceeds v_c, an additional peak appears in the NMR spectrum. This maximum originates in ^{3}He-B from a plateau in $\beta(r)$ since β defines the NMR frequency f according to the formula $f^2\simeq f_0^2+f_L^{\beta 2}\sin^2\beta$, where f_0 is the Larmor frequency and f_L^β is the temperature-dependent longitudinal resonance frequency. The effect of superflow can also be seen in the frequency of spin-wave modes localized at the center of the flare-out texture.

Figure 1 displays the measured spin-wave frequencies at 284 Oe in a vortex-free state up to ± 0.3 rad/s. The spacing is clearly different for opposite directions of rotation. This difference was not connected with the relative directions of $\mathbf{H}$ and $\boldsymbol{\Omega}$ as for the gyromagnetic effect caused by vortices.[10] On the contrary, the sign of the difference, i.e., the direction of rotation yielding the larger frequency shift, seemed to vary randomly from one cooldown to another. A switchover between the

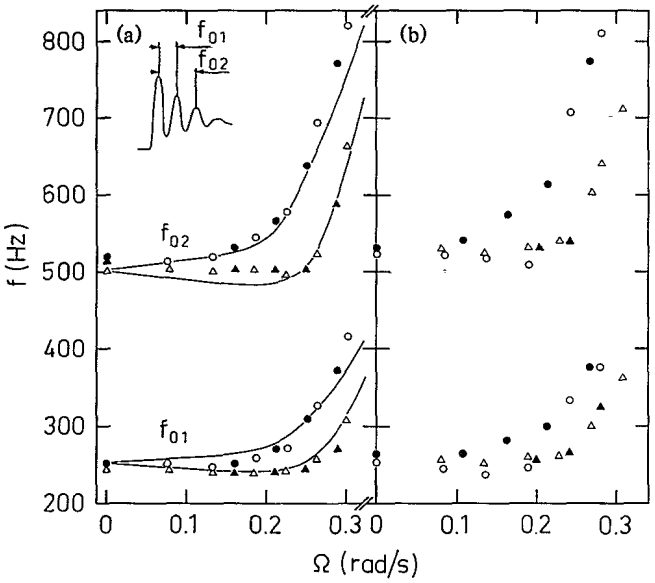

FIG. 1. (a) Spin-wave spacings f_{01} and f_{02} (defined in the inset) as a function of Ω measured at $H=284$ Oe, $p=29.3$ bars, and $T=0.48T_c$. The data display a large-shift branch (open and filled circles) and a small-shift branch (open and filled triangles). These branches correspond to different directions of rotation, but the direction yielding a specific branch varies randomly from one cooldown to another. Open and closed symbols refer to accelerating and decelerating rotation speed, respectively. Solid curves based on theoretical calculations are discussed in the text. (b) Spin-wave spacing measured at $0.46T_c$ showing a transition from the small-shift branch to the large-shift branch during acceleration (follow the open circles).

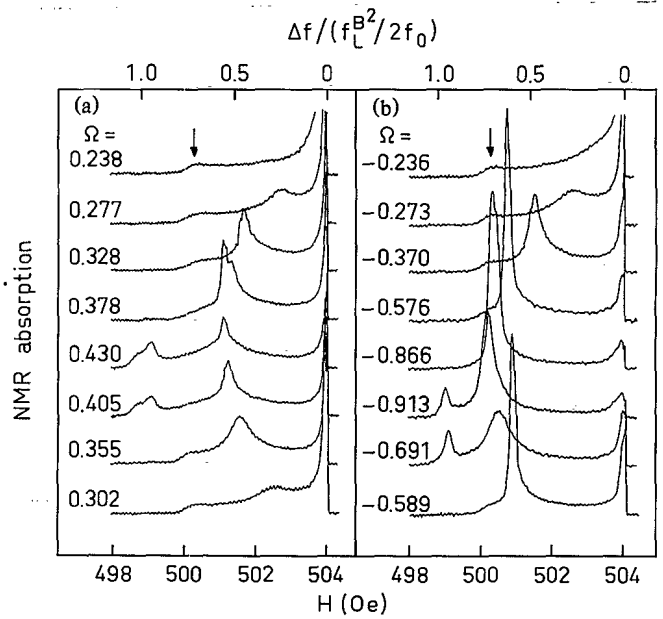

FIG. 2. Two Ω sequences of NMR spectra recorded at 29.3 bars and at $0.65T_c$ as a function of magnetic field in (a) one direction of rotation and in (b) the opposite direction. The scaled frequency shift $\Delta f/(f_L^{B2}/2f_0)$ is shown at the top of the figure. The arrows denote the high-frequency edge of the flare-out texture spectrum, the shift of which is displayed in Fig. 4.

branches was observed during one experiment as shown in Fig. 1(b). The spacing between the spin waves diminished and their damping increased strongly with temperature, and, therefore, the sensitivity was not good enough to study these direction-dependent effects near T_c. Toward lower temperatures, the difference in the spacing rapidly decreased and could not be resolved below $T=0.4T_c$ before vortices entered the sample at about 0.4 rad/s.

The randomness in the sign of the observed effects immediately rules out an explanation with bulk intrinsic orbital angular momentum, as well as an explanation with the surface current due to orbital angular momentum. With our experimental accuracy, neither could we find any smaller effect, with proper transformation properties under reversal of **H** and **Ω**, which could be assigned to intrinsic orbital angular momentum. To obtain some quantitative results from the measured data we adopt the viewpoint that the observed effects are due to flow-magnetized surfaces producing F_{gm}^s, although it is not clear to us how the random sign will fit into this picture.

The solid lines in Fig. 1(a) are theoretical curves calculated for surface magnetization $|\kappa_s| \simeq 300\Omega$ Oe s. The boundary condition was first obtained by minimization of F_s and F_{gm}^s; the texture was then calculated by use of $\xi_H/R=0.27$, which yields the slope of $\beta(r)\simeq\beta_1 r$ in the center of the cylinder. According to the harmonic approximation, the spin-wave spacing is directly proportional to β_1. The fit also yields the value $v_c=0.37$ mm/s at $T=0.48T_c$.

Figure 2 displays typical data measured at 504 Oe by a gradual increase or decrease of the speed of rotation by steps of 0.05 rad/s once every 5 min. In this manner, essentially vortex-free states up to 0.9 rad/s could be generated—at 284 Oe, the same acceleration procedure resulted in vortex creation already at 0.4–0.5 rad/s. Our data show completely different behavior for opposite directions of rotation. Again, as in the case of spin waves, the direction of rotation that yielded a particular sequence of spectra, such as illustrated in Fig. 2, seemed to depend randomly on the cooldown, and not on the relative orientation of **H** and **Ω**.

Both directions of rotation display a first-order textural transition. In Fig. 2(a), rotation induces a transition at $\Omega=0.4$ rad/s and, in Fig. 2(b), at $\Omega=0.9$ rad/s in the opposite direction of rotation; they are clearly seen in the NMR spectra as a shift of the absorption to lower fields. During deceleration the transitions back to the original state occur at 0.37 and 0.60 rad/s. The precise values of the angular velocity for these transitions differ slightly from run to run, presumably depending on the actual texture in the cell and on varying "vortex leakage" dur-

ing acceleration. The counterflow states were stable for several hours. The stability of the large counterflows at 0.7 rad/s was also studied by sweeping of the temperature. On the basis of earlier persistent-current experiments[11] one could anticipate a discontinuity in the counterflow, but it was not observed. At 0.9 rad/s the heat flow during the temperature sweep easily destroyed the counterflow state.

The calculation of Ref. 9 explains qualitatively the observed spectra, but our measurements show a much richer behavior than expected. A striking difference, in addition to the observed first-order textural transition, is the presence of single, double, and triple maximum peaks in the shifted main absorption line at high rotation speeds; the calculation predicts only double maximum peaks.

We have repeated the calculation of Ref. 9 and find that, during a large counterflow, $\alpha(r)$ is very sensitive to its value at the boundary; A decrease by a few degrees from 60° will change the value of α in the center of the cell from $\sim 130°$ to $\sim -50°$. This change, in turn, affects $\beta(r)$ and would be seen as a shift in the NMR line toward higher frequencies; but this line, too, would have a double maximum. The only way, as far as we can find, to produce a single maximum peak is for the Leggett angle $\Theta = 104°$ to have opposite signs on the boundary and in the bulk liquid. The large change in α close to the wall would then be absent and $\beta(r)$ could be monotonic, resulting in a single maximum for the shifted NMR line.

Even though there is no exact agreement between the measured and calculated line shapes, there is still good agreement between the calculated and measured NMR frequency shifts. Figure 3 displays the scaled NMR frequency shift as a function of Ω for the counterflow-induced peak in the spectra of Fig. 2. The data are fitted nicely by the theoretical curve showing the higher frequency of the calculated double maximum peak.[9] This fit yields $v_c = 0.40$ mm/s at $T = 0.65T_c$, which is close to the value obtained from the spin-wave spacing. If we take into account the calculated[8] temperature dependence of v_c, our data give $v_c = 0.70$ mm/s at T_c, which is below the theoretical estimate of 1.0 mm/s in the Ginzburg-Landau region. To compare our data with the results of Hutchins, Brewer, and Kruppa,[2] we also measured the dipolar critical velocity at 5 bars and obtained $v_c = 0.20$ mm/s at $0.80T_c$. This is 100% larger than the value of Ref. 2 but, still, it is only about 60% of the theoretical estimate.

By inspecting the measured line shapes we may conclude that the observed first-order textural transition is due to an abrupt change in the boundary condition for the $\hat{\mathbf{n}}$ vector. This interpretation relies on the fact that the NMR response for either a planar or a coaxial $\hat{\mathbf{n}}$ soliton [a single peak at $\Delta f/(f_L^{B2}/2f_0) = 1$] does not agree with the observed peaks which appear above the transition. The change in the boundary condition takes place at velocities which must be too small to modify the actual surface structure,[12] and therefore we believe that it is a consequence of an intricate competition between various surface and bulk free-energy terms which have to be minimized together to explain the transition quantitatively.

Small changes in the boundary condition for the $\hat{\mathbf{n}}$ vector can be observed already at low rotation speeds in the data of Fig. 2. The value of β at the boundary defines the high-frequency edge in the NMR spectrum of the flare-out texture (see the arrows in Fig. 2). In the measured spectra, there is an obvious increase in the frequency shift of the edge in the rotating state, which is displayed as a function of Ω in Fig. 4.

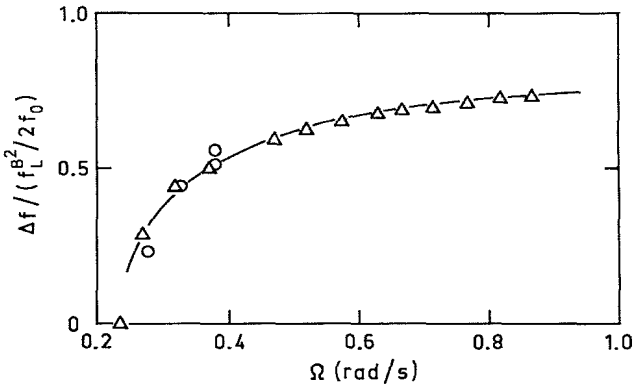

FIG. 3. Scaled NMR frequency shift as a function of Ω for the flow-induced maximum in the spectra of Fig. 2; circles and triangles display results at positive and negative directions of rotation, respectively. Data below the textural transition only are displayed. The two circles at 0.38 rad/s are due to the double-peak structure of the absorption maximum.

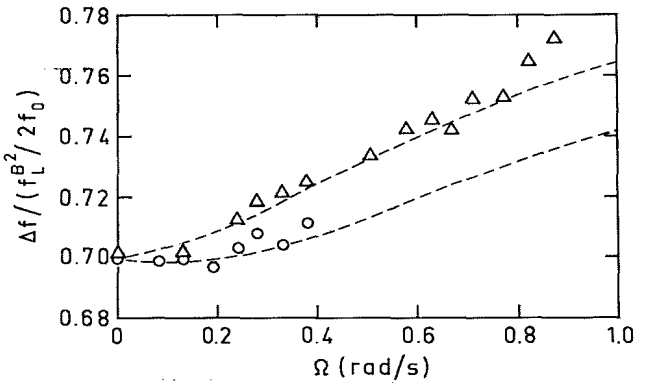

FIG. 4. The scaled frequency shift of the high-frequency tail of the data in Fig. 2 as a function of rotation speed: circles and triangles represent positive and negative directions of rotation, respectively. The frequency shift was determined from the falling edge of the signal (denoted by arrows in Fig. 2), which can be determined only at speeds not causing the transition in the boundary condition. The dashed curves are discussed in the text.

The behavior in Fig. 4 can be understood by the use of a simple model. We minimize $F_s+F_{gm}^s$, in the case of $\hat{\mathbf{s}}\perp\mathbf{H}$ and $\mathbf{v}_s\perp\mathbf{H}$, together with an approximate bulk liquid energy within ξ_H from the wall comprised of

$$F_M+F_{vH}\simeq\xi_H/(d/a)d\sin^2\beta[1-(\Omega R/v_c)^2(1-\tfrac{5}{8}\sin^2\beta)],$$

where $d/a\simeq 2.5$ mm.[13] We thus neglect the variation in α and obtain for the minimum simply

$$\sin^2\beta=\frac{4}{5}\left[1-\frac{(4\kappa_s/5H+Q}{\frac{5}{2}+Q(\Omega R/v_c)^2}\right],$$

where the phenomenological $Q=\xi_H/(d/a)$ can be obtained by fitting the calculated curve to the experimental data. The dashed lines in Fig. 4 give the frequency shift according to the above model with $Q=0.31$, $\kappa_s=50\Omega$ Oe s, and $v_c=0.80$ mm/s. On the basis of this analysis, we have used the shift of the high-frequency tail to determine $|\kappa_s|$ which yielded values from 50Ω to 150Ω Oe s for T/T_c between 0.53 and 0.65.

In conclusion, we have observed direction-dependent rotation effects in the flare-out texture without vortices. These results show large modifications in the B-phase boundary condition under relatively small flows of the order of 1 mm/s. We have analyzed these effects using a surface energy term $\frac{4}{5}\kappa_s a\hat{\mathbf{\Omega}}\cdot\mathbf{R}\cdot\mathbf{H}$ and obtained values for κ_s with puzzling random sign. No trace of the bulk intrinsic orbital angular momentum of ^{3}He-B in a magnetic field could be deduced.

We are grateful to Yu. M. Bunkov, O. Magradze, and G. E. Volovik for contributions at various stages of this work, and to H. E. Hall, O. V. Lounasmaa, and M. M. Salomaa for useful discussions. This work was supported, under the auspices of the ROTA project, by the Academy of Finland and by the Academy of Sciences of the U.S.S.R. A scholarship from the Emil Aaltonen Foundation is gratefully acknowledged by one of us (K.K.N.).

[1]P. J. Hakonen, O. T. Ikkala, S. T. Islander, and O. V. Lounasmaa, J. Low Temp. Phys. **53**, 425 (1983).

[2]J. Hutchins, D. F. Brewer, and D. Kruppa, Phys. Rev. Lett. **55**, 1410 (1985).

[3]A. L. Fetter, J. Low Temp. Phys. **23**, 245 (1976).

[4]W. F. Brinkman and M. C. Cross, in *Progress in Low Temperature Physics,* edited by D. F. Brewer (North-Holland, Amsterdam, 1978), Vol. 7A, p. 106.

[5]T. Dombre and R. Combescot, Phys. Rev. B **32**, 1751 (1985); S. Yip, J. Phys. C **19**, 1491 (1986).

[6]G. E. Volovik and V. P. Mineev, Zh. Eksp. Teor. Fiz. **86**, 1667 (1984) [Sov. Phys. JETP **59**, 972 (1984)]; P. Muzikar, in *Proceedings of the Seventeenth International Conference on Low Temperature Physics, Karlsruhe, West Germany, 1984,* edited by U. Eckern *et al.* (North-Holland, Amsterdam, 1984), Vol. 1, p. 45; V. P. Mineev, Zh. Eksp. Teor. Fiz. **90**, 1236 (1986) [Sov. Phys. JETP **63**, 721 (1986)].

[7]Actually, this was tried but the frozen-in texture and textural defects rendered the trial impossible.

[8]P. J. Hakonen, M, Krusius, M. M. Salomaa, R. H. Salmelin, J. T. Simola, A. D. Gongadze, G. E. Gurgenishvili, and G. A. Kharadze, to be published, and references therein.

[9]G. E. Volovik, A. D. Gongadze, G. E. Gurgenishvili, G. A. Kharadze, and M. M. Salomaa, Pis'ma Zh. Eksp. Teor. Fiz. **36**, 404 (1982) [JETP Lett. **36**, 489 (1982)].

[10]P. J. Hakonen, M. Krusius, M. M. Salomaa, J. T. Simola, Yu. M. Bunkov, V. P. Mineev, and G. E. Volovik, Phys. Rev. Lett. **51**, 1362 (1983).

[11]J. P. Pekola, J. T. Simola, P. J. Hakonen, M. Krusius, O. V. Lounasmaa, K. K. Nummila, G. Mamniashvili, R. E. Packard, and G. E. Volovik, Phys. Rev. Lett. **53**, 584 (1984).

[12]E. V. Thuneberg, Phys. Rev. B **33**, 5124 (1986).

[13]D. D. Osheroff, Physica (Amsterdam) **90B**, 20 (1977).